Sonographic Evaluation of Plantar Hindfoot and Midfoot Pain

Douglas Hoffman, MD, Stefano Bianchi, MD

Plantar hindfoot and midfoot pain is a common orthopedic condition. Plantar fasciopathy is the most common cause of plantar foot pain, and sonographic evaluation can easily show the characteristic pathologic changes. In addition, sonography is well suited to evaluate other potential causes of plantar foot pain. We present a review of the sonographic findings of plantar fasciopathy and other potential causes of plantar hindfoot and midfoot pain.

Key Words—hindfoot; midfoot; plantar fasciopathy; sonography

Foot pain is a common orthopedic condition, with a prevalence of 1 per 4 to 1 per 5 people in population-based studies.[1–3] Although plantar fasciopathy is the most common cause of plantar hindfoot pain presenting to outpatient clinics,[4] several other disorders can present as plantar foot pain and should be considered as part of the differential diagnosis. The evaluation of plantar foot pain begins with a careful history, physical examination, and standard radiographs. In cases in which the patient's symptoms become refractory to treatment or the cause of the patient's symptoms is unclear, more advanced imaging may be indicated. Sonographic evaluation of the plantar aspect of the foot can easily show the characteristic pathologic changes associated with plantar fasciopathy.[5–8] In addition, when the plantar fascia appears normal on sonography, a systematic examination of both hindfoot and midfoot structures that may explain an alternative cause of pain is warranted. This pictorial essay shows the classic sonographic findings of plantar fasciopathy and other foot disorders that should be considered in patients with plantar foot pain.

Received October 18, 2012, from the Department of Orthopedics, Essentia Health, Duluth, Minnesota USA (D.H.); and Cabinet Imagerie Médicale, Geneva, Switzerland (S.B.). Revision requested November 6, 2012. Revised manuscript accepted for publication November 30, 2012.

Address correspondence to Douglas Hoffman, MD, Department of Orthopedics, Essentia Health, 400 E Third St, Duluth, MN 55804 USA.

E-mail: douglas.hoffman@essentiahealth.org

Abbreviations
MR, magnetic resonance

doi:10.7863/ultra.32.7.1271

Abnormalities of the Plantar Aponeurosis

The plantar aponeurosis is composed of 3 cords: medial, central, and lateral. The central cord is the largest and strongest, taking its origin from the medial tubercle of the calcaneus and dividing into 5 diverging bands, which insert onto the plantar plates of the metatarsophalangeal joints and the bases of the proximal phalanges. The lateral cord originates from the lateral calcaneal tubercle, travels superficial to the abductor digiti minimi, and inserts onto the base of the fifth metatarsal, inferior and lateral to the attachment of the peroneus brevis. The thin medial cord, the least clinically important of the 3 cords, also arises from the medial calcaneus, overlies the abductor hallucis muscle, and blends distally with its fascia.

Both the lateral and central cords of the plantar aponeurosis are readily evaluated by sonography. The central cord appears as a uniformly hyperechoic fibrillar structure that is thick and triangular proximally and thin as one scans distally.[7] The normal sonographic plantar fascia thickness measured at its widest point is approximately 3 to 4 mm.[8] At its origin on the calcaneal tuberosity, the deepest and most posterior fibers of the aponeurosis take an oblique course at their bony attachment, which may appear hypoechoic as a result of anisotropy. Lateral cord disorders most often occur at its insertion onto the base of the fifth metatarsal, where it is easily evaluated by sonography. The lateral cord is visualized as a thin band that abruptly widens at its insertion, maintaining a uniform hyperechoic fibrillar echo texture throughout its course.

Plantar Fasciopathy

Plantar fasciopathy most commonly involves the proximal third of the central cord of the plantar aponeurosis (Figure 1).[6–9] Characteristic sonographic findings of plantar fasciopathy include a thickened hypoechoic central cord with loss of the normal fibrillar pattern at the proximal third and its insertion onto the medial tubercle of the calcaneus.[9] Hypoechoic foci may be present within the thickened aponeurosis, reflecting focal areas of collagen necrosis and myxoid degeneration.[10] Other findings include blurring of the deep and superficial borders of the aponeurosis, perifascial edema, and cortical irregularity of the calcaneus, often with a traction osteophyte (enthesophyte).[5,7] Doppler imaging may reveal hyperemia both within the proximal plantar aponeurosis and in the surrounding tissue.[11]

Figure 1. Plantar fascia enthesopathy. **A** and **C**, Long-axis sonogram (**A**) and corresponding T2-weighted fat-suppressed MR image (**C**) of the proximal plantar fascia. In **A**, sonography shows a thickened hypoechoic aponeurosis (black arrowhead) with loss of the normal hyperechoic fibrillar pattern. Note the cortical irregularity of the underlying cortex of the calcaneus and the blurring of the deep and superficial margins of the aponeurosis compared with the normal aponeurosis more distally (curved white arrow). **B** and **D**, Short-axis sonogram (**B**) and corresponding T2-weighted fat-suppressed MR image (**D**) of the proximal plantar fascia. In **B**, note a focal hypoechoic area (black arrowheads) of the preinsertional medial cord of the plantar fascia. The lateral cord has a normal appearance in both images (white arrowheads).

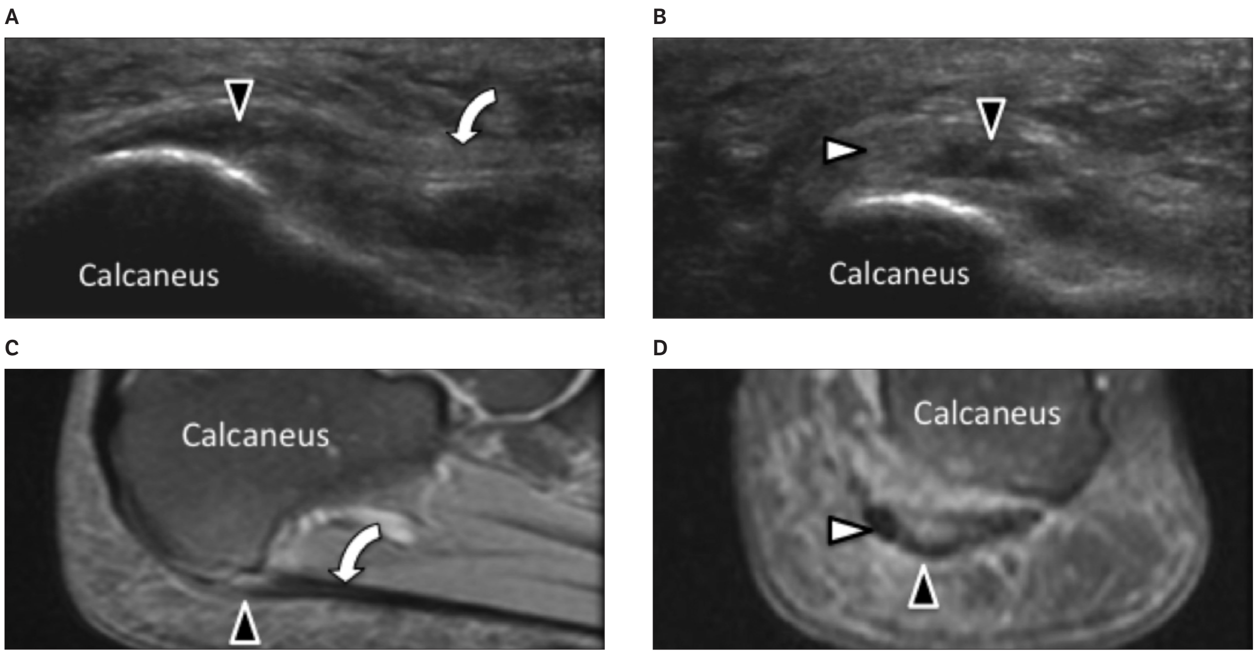

Less commonly, plantar fasciopathy may occur at the middle or distal third of the plantar aponeurosis and recently has been associated with recalcitrant plantar heel pain (Figure 2).[9]

Plantar Fascia Tears

Acute tears of the plantar fascia can occur both at its proximal third (Figure 3A) and at the midsubstance (Figure 3B). The sonographic appearance includes focal nodular thickening of the plantar fascia with loss of fibrillar continuity often affecting the superficial fibers more than the deep ones.[6] Surrounding edema may be present depending on the acuteness of the injury. Correlation with the patient's history is helpful in differentiating a partial tear from severe fasciopathy, although considerable overlap exists between the two entities. A traumatic onset of acute pain after a snapping sound, particularly in a patient with preexisting plantar fasciopathy, or a recent local steroid injection into the plantar fascia increases the likelihood of a plantar fascia tear.[12] In cases in which a complete tear of the aponeurosis is less obvious, dynamic evaluation by gently dorsiflexing

Figure 2.Plantar fasciitis: midsubstance. **A** and **B**, Long-axis sonograms at the midsubstance of the plantar aponeurosis show a segment of hypoechoic thickening, loss of the internal fibrillar echo texture, and blurring of the margins (black arrowheads) characteristic of plantar fasciitis. Note the normal thickness and appearance of both the proximal and distal portions of the plantar aponeurosis (white arrowheads). In **A**, the distance of the pathologic segment of the plantar aponeurosis from its calcaneal insertion (dashed double arrow) can be measured, which can accurately guide a local injection or shock wave treatment.

A B

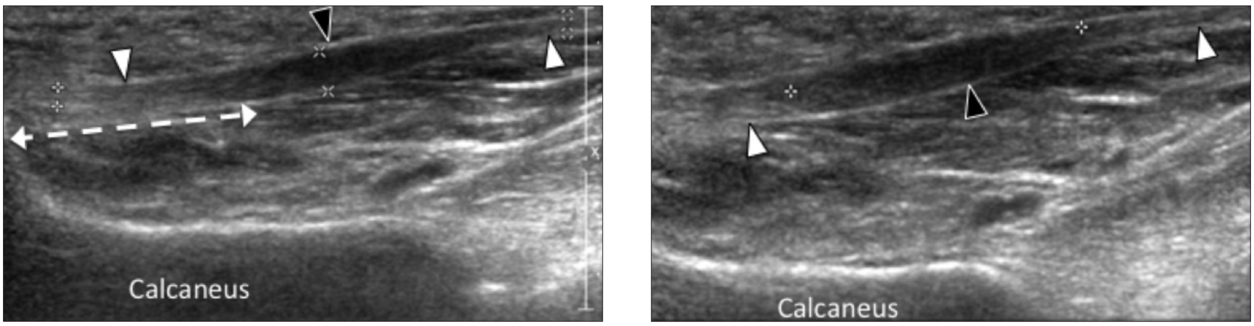

Figure 3. Plantar fascia tear. **A**, Long-axis sonogram shows a retracted (white arrowhead) central band of the plantar aponeurosis (calipers) from its calcaneal attachment with interposing and surrounding edema and hemorrhage (black arrowhead). Note the progressive thickening and subtle loss of the fibrillar echo texture of the aponeurosis distal to the rupture, suggestive of underlying plantar fasciitis before rupture. **B** and **C**, Long-axis sonogram (**B**) and corresponding T1-weighted MR image (**C**) in a different patient show rupture of the central third of the plantar aponeurosis. Both the proximal and distal ends of the aponeurosis (white arrowheads) are thickened, indicative of preexisting plantar fasciitis. Note the complete discontinuity of the aponeurotic echo texture at the site of rupture (black arrowheads).

A C

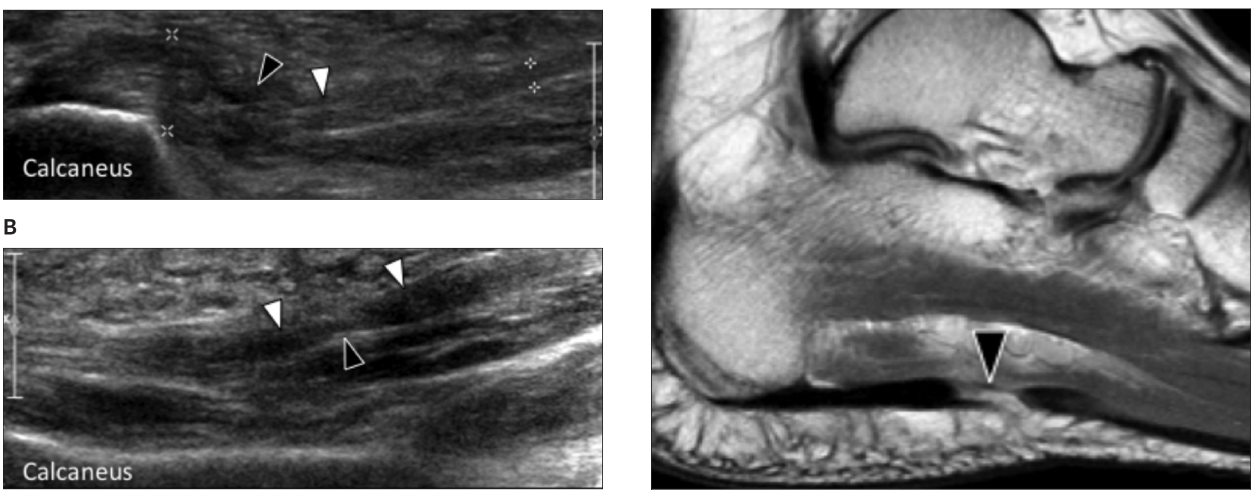

the ankle and great toe can help distinguish high-grade plantar fasciopathy or a partial tear from that of a full-thickness tear by showing discontinuity of movement or separation between the proximal and distal ends of the aponeurosis.

Enthesopathy of the Lateral Cord of the Plantar Fascia

Enthesopathy of the lateral cord of the plantar fascia may present as either lateral or plantar foot pain. It often coexists with plantar fasciopathy because patients may walk on the lateral aspect of their foot to avoid direct pressure on the medial tubercle of the calcaneus. The lateral cord of the plantar fascia inserts onto the inferior aspect of the base of the fifth metatarsal and has a much broader attachment than that of the peroneus brevis tendon, which inserts onto the lateral aspect of the metatarsal (Figure 4A). Knowledge of these attachments facilitates differentiation of lateral cord enthesopathy from preinsertional tendinopathy of the peroneus brevis. Sonograms of enthesopathy reveal hypoechoic thickening and loss of the fibrillar architecture at its insertion (Figure 4B). In cases in which these changes are subtle, comparison with the contralateral side is imperative. Color Doppler imaging may reveal hyperemia in more acute cases. Often, the pressure of the ultrasound transducer reproduces the pain, confirming the diagnosis.

Plantar Fibromatosis (Ledderhose Disease)

Plantar fibromatosis is a benign fibroblastic proliferative disorder characterized by idiopathic focal nodules of the plantar fascia most often occurring in patients aged 30 to 50 years, but it may occur at any age, including in children.[13] The most common presentation is a painless nodule on the medial longitudinal arch that is multiple in 33% of cases and occurs bilaterally 20% to 50% of the time.[13] In patients who are symptomatic, pain is due to direct pressure against a large nodule, pressure of the nodule against the medial plantar nerve, or inflammation within the nodule. Characteristic sonographic findings include discrete hypoechoic or mixed echogenic fusiform nodular thickening of the

Figure 4. Enthesopathy of the lateral cord of the plantar fascia. **A**, Long-axis sonogram shows the insertion of the normal peroneus brevis (curved white arrow) onto the base of the fifth metatarsal, which is superior to that of the lateral band of the plantar fascia. In addition, the peroneus brevis does not broaden at its bony attachment in contrast to the lateral band. **B**, Long-axis sonogram obtained over the lateral band of the plantar fascia shows that it is thickened and hypoechoic with loss of the fibrillar echo texture at its attachment site (black arrowheads). Note the transition from the normal echo texture (white arrowhead) to abnormal at its insertion, indicative of enthesopathy.

A

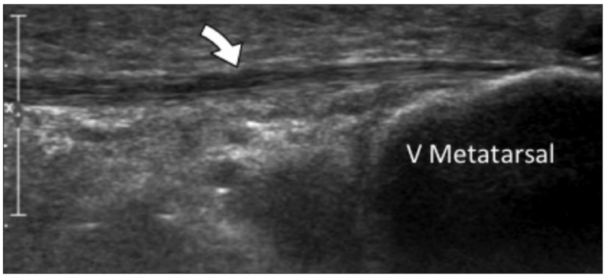

B

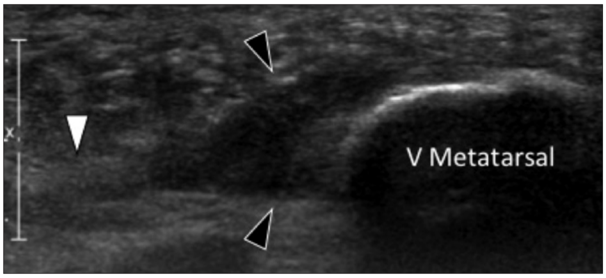

Figure 5. Inflammatory plantar fibromatosis. **A**, Long-axis sonogram shows a large fusiform hypoechoic nodule (black arrowheads) within the plantar aponeurosis. Note the normal deep flexor hallucis longus tendon (curved white arrow). No adhesions between the tendon and the nodule were detected with dynamic examination. **B**, Long-axis sonogram from the same patient shows color Doppler activity (white arrowheads), indicative of an inflammatory nodule.

A

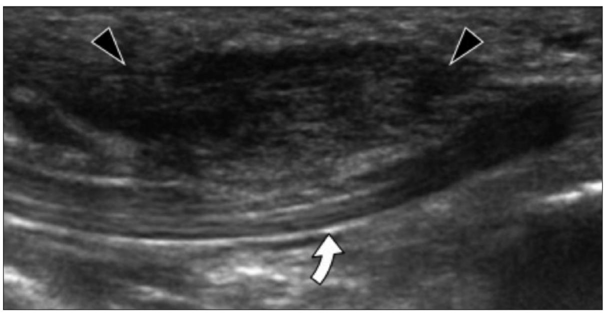

B

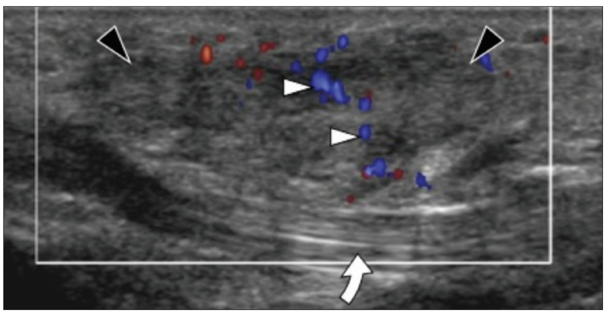

superficial plantar aponeurosis involving the medial (60%) or central (40%) portion of the aponeurosis (Figure 5).[13,14] Symptomatic nodules may reveal intralesional hypervascularity (Figure 5A).[14] Contiguity of the nodule with the plantar fascia distinguishes it from other soft tissue tumors.

Calcaneal Stress Fracture

A stress or fatigue fracture of the calcaneus should be considered in any individual presenting with plantar hindfoot pain. The diagnosis is usually confirmed by characteristic radiographic findings. In cases in which radiographic findings are normal, magnetic resonance (MR) imaging is definitive. Evaluation of the calcaneal cortex should be a routine part of the sonographic evaluation of heel pain. The presence of irregularity of the calcaneal cortex with an adjacent hypoechoic stripe, representing thickening and edema of the periosteum, and increased vascularity should raise the suspicion of a stress fracture and prompt further imaging (Figure 6).[15,16]

Medial Tarsal Tunnel Syndrome

Entrapment of the tibial nerve or its branches within the tarsal tunnel is referred to as tarsal tunnel syndrome. Tarsal tunnel syndrome is an important cause of plantar foot pain and has been implicated as the cause of intractable chronic heel pain.[17] Specific causes of tarsal tunnel syndrome can be identified in approximately 60% to 80% of cases and include foot deformities, space-occupying lesions, trauma, tumors, and tenosynovitis of the tendons within the tarsal tunnel.[18] Sonography is well suited for evaluation of potential causes of tarsal tunnel syndrome and should be routinely performed in the evaluation of plantar foot pain.[19] In addition, sonography can guide diagnostic or therapeutic procedures in select cases.

Talocalaneal Coalitions

Talocalaneal coalitions account for 45% of all tarsal coalitions and most commonly involve the middle facet of the subtalar joint.[20] Sonography can suggest the presence of a coalition by revealing a prominent irregular bony outline, or beak-shaped appearance, of the medial talus overlying the sustentaculum tali rather than its normal rounded contours (Figure 7, A and B). The medial plantar nerve runs adjacent to the medial talocalcaneal joint, thus rendering it susceptible to entrapment neuropathy from a talocalcaneal coalition (Figure 7C). Sonography has two advantages in assessing for medial plantar nerve compression. First, long- and short-axis images over the pathologic segment of the nerve can be accurately obtained under real-time scanning. Second, dynamic examination during movements of the ankle and local sonographically guided compression help in confirming the diagnosis by reproducing the patient's symptoms. Clinically, a positive Tinel sign at the bony prominence of the talocalcaneal coalition should alert the sonographer as to the possibly of medial plantar nerve compression. When a talocalcaneal coalition is suspected on sonography, MR imaging or computed tomography is necessary to confirm its presence and further assess the details of the coalition.[21]

Ganglion Cysts

Ganglia within the tarsal tunnel are well described as a cause of tarsal tunnel syndrome.[22] They may also coexist with talocalcaneal coalitions.[19] Most commonly, ganglia within the tarsal tunnel arise from either the talocalcaneal or talocrural joint.[22] Compression of the tibial nerve in the proximal tarsal tunnel or the medial plantar nerve more distally is not uncommon (Figure 8).[19,22] Sonographically, ganglia appear as well-demarcated masses that range from

Figure 6. Calcaneal stress fracture. **A**, Long-axis color Doppler sonogram of the plantar medial cortex of the calcaneus shows hyperechoic thickening of the calcaneal cortex with adjacent hypoechoic thickening of the periosteum. Color Doppler imaging reveals markedly increased vascularity of the periosteum (white arrowheads). **B**, Corresponding gadolinium-enhanced sagittal T1-weighted MR image shows a fracture line (black arrows) within the body of the calcaneus, characteristic of a stress fracture.

A

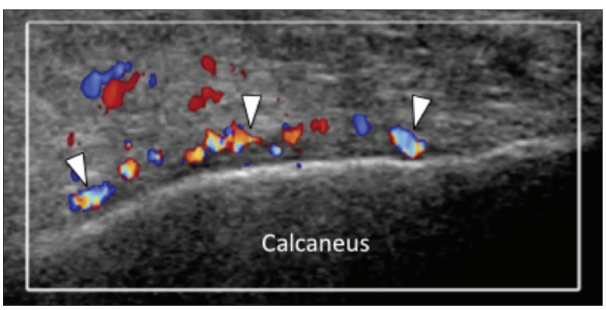

B

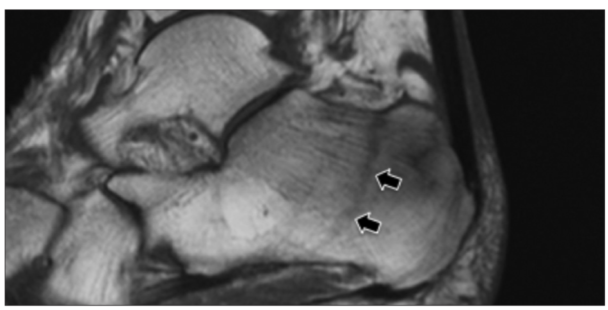

completely anechoic to hypoechoic with multiple internal septations and always without internal vascularity.[22,23] Nonpalpable occult ganglia are also accurately revealed by sonography.[19] Real-time sonographically guided aspiration can confirm the diagnosis, reduce the pressure of the ganglion on the nerve, and decrease patient discomfort.

Figure 7. Talocalcaneal coalition with compression of the medial plantar nerve. **A** and **B**, Coronal oblique sonogram obtained at the level of the sustentaculum tali (**A**) and corresponding T1-weighted MR image (**B**) show a fibrous coalition (white arrow) between the talus and sustentaculum tali (ST). Note the beak-shaped bony prominence (white arrowhead) due to the coalition. **C**, Long-axis sonogram over the medial plantar nerve shows displacement and enlargement (black arrowheads) from the talocalcaneal coalition (white arrow). Note the transition from a normal appearance of the nerve more proximally (white arrowhead) to an enlarged and hypoechoic nerve as it becomes displaced by the coalition.

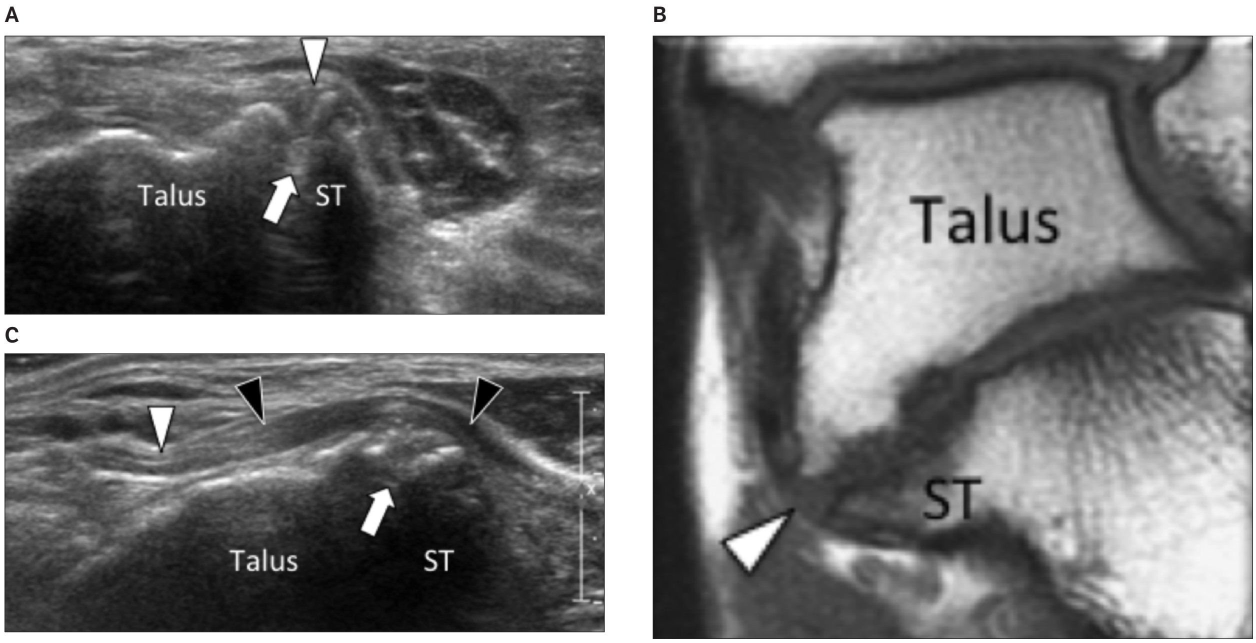

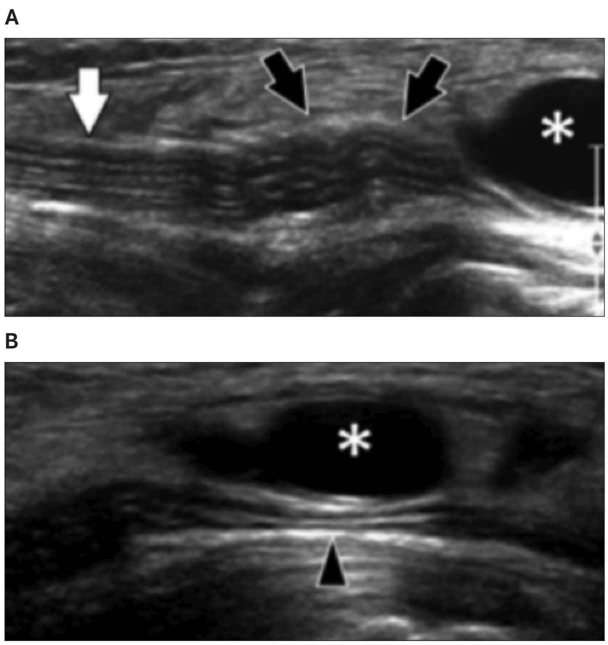

Figure 8. Tarsal tunnel ganglia. **A**, Long-axis sonogram of the medial tarsal tunnel shows an anechoic ganglion (asterisk) compressing the tibial nerve. The proximal portion of the tibial nerve (white arrow) is normal in appearance, whereas the nerve just proximal to the ganglion (black arrows) has a wrinkled appearance due to the compression. **B**, Long-axis sonogram of a ganglion more distal in the medial tarsal tunnel (asterisk) shows compression of the medial plantar nerve (black arrowhead). **C**, Long-axis color Doppler sonogram from the same patient as in **B** shows no vascularity within the ganglion.

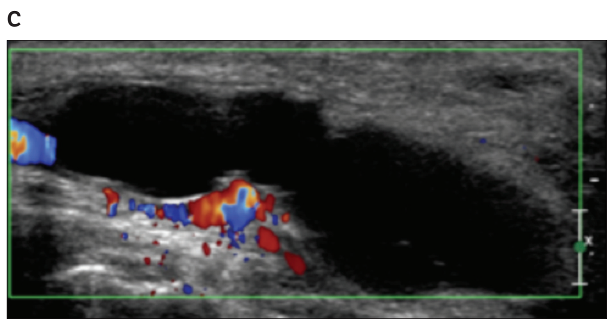

Trauma

Trauma to the medial side of the ankle may result in tarsal tunnel syndrome. Injury to the posterior tibial nerve or its branches may result from direct trauma, either a direct blow or a penetrating injury (Figure 9), or indirect trauma, resulting in traction neuropraxia (Figure 10). Trauma may also cause damage to other structures within the tarsal tunnel, eg, fracture or tendon injury, resulting in either direct compression to the nerve or indirect compression from excessive swelling.

Tumors

Both benign and malignant tumors have been reported to occur within the tarsal tunnel.[24] On sonography, tumors appear as hypoechoic or hyperechoic focal masses and are easily distinguished from simple ganglion cysts. The relationship with a nerve is the most useful finding in diagnosing nerve sheath tumors such as a schwannoma or neurofibroma (Figure 11). The sonographic appearance of other tumors is nonspecific (Figure 12).

Figure 9 Glass fragment resulting in a tear of the medial plantar nerve. **A**, Short-axis sonogram of the medial tarsal tunnel shows the glass fragment (black arrowheads) with a posterior reverberation artifact (white arrowhead). **B**, Long-axis sonogram from the same patient shows the normal proximal nerve (curved white arrow) with the stump neuroma (black arrow) located just proximal to the glass fragments (black arrowheads).

A

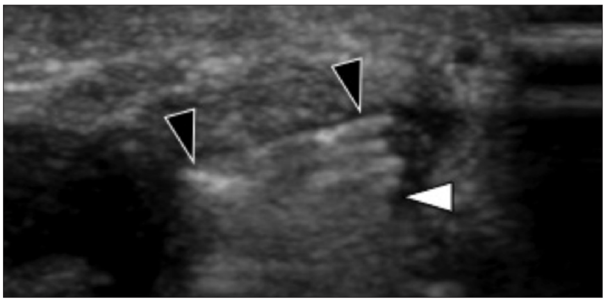

B

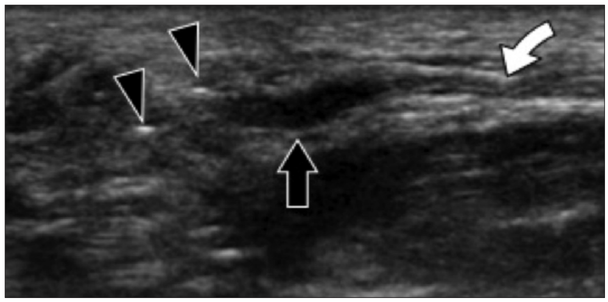

A

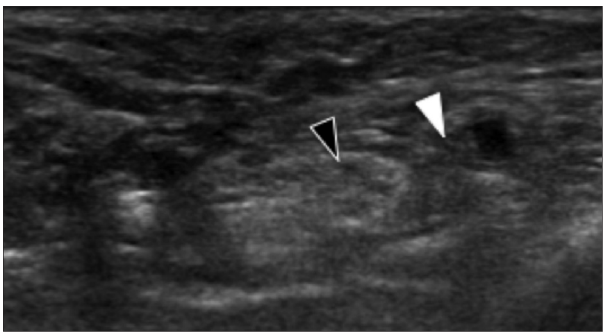

Figure 10 Traumatic tear of the medial plantar nerve. **A** and **B**, Short-axis sonograms taken at points A and B in **C**. In **A**, the medial plantar nerve (white arrowhead) is visualized at the level where the tear begins (white arrowhead). The lateral plantar nerve is adjacent (black arrowhead). In **B**, there is only a hypoechoic gap (white arrow) between the two ends of the tear. The black arrowhead indicates the lateral plantar nerve. **C**, Long-axis sonogram shows the two ends of the medial plantar nerve (white arrows), revealing the extent of the hypoechoic gap from the tear next to a normal lateral plantar nerve (black arrowheads).

B

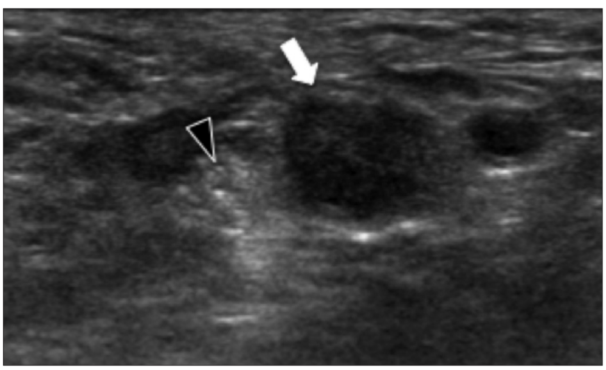

C

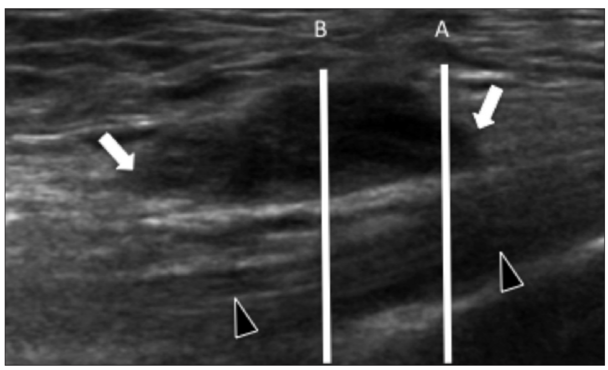

The presence of vascularization, inhomogeneity, poor bordering, broad contact with the underlying fascia, or invasion of bone or neurovascular bundles suggests a possible malignancy and necessitates further imaging, biopsy, or both.[14]

Compression of the Nerve to the Abductor Digiti Minimi Muscle

Chronic compression of the first branch of the lateral plantar nerve to the abductor digiti minimi muscle, also termed Baxter neuropathy, should be considered in the differential diagnosis of chronic plantar foot pain and may either be present

Figure 11. Tarsal tunnel schwannoma of the posterior tibial nerve. **A** and **C**, Short-axis color Doppler sonogram (**A**) and corresponding T2-weighted MR image (**C**) through the proximal tarsal tunnel. In **A**, the schwannoma appears as a hypoechoic well-demarcated rounded mass (black arrowheads) adjacent to the posterior tibial artery and veins (curved white arrow). In **C**, the T2-weighted MR image reveals the schwannoma as a hyperintense nodule abutting the muscle and tendon of the flexor hallucis longus. **B** and **D**, Long-axis sonogram (**B**) and corresponding proton density–weighted MR image (**D**). In **B**, the sonogram shows the hypoechoic schwannoma (black arrowhead) within the posterior tibial nerve (white arrowheads), which shows a normal fascicular pattern. Superficial to the nerve is the posterior tibial artery (curved arrow). In **D**, note the schwannoma (black arrowhead) within the normal nerve (white arrowheads).

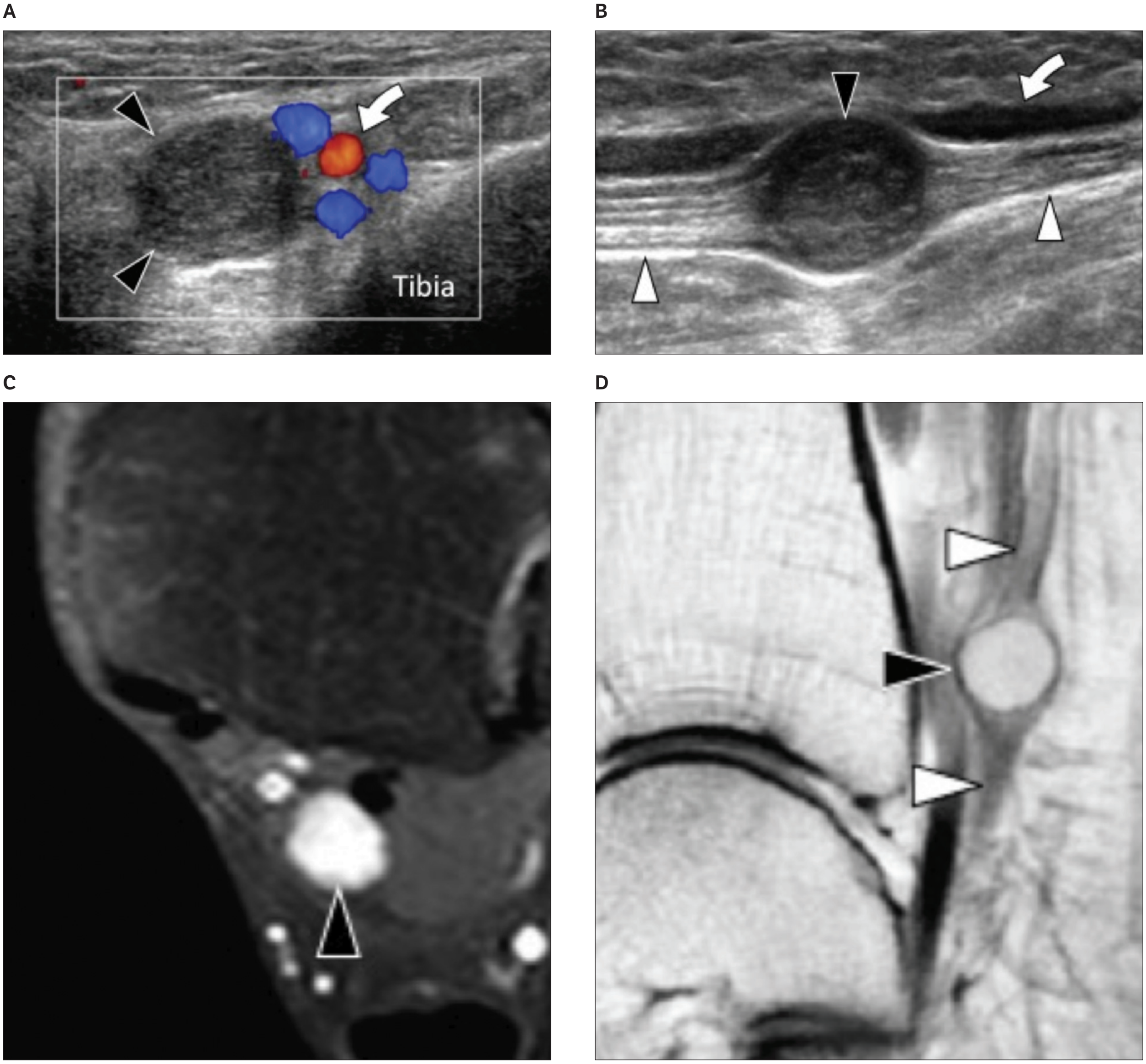

as an isolated finding or coexist with plantar fasciopathy.[25] Although direct compression of the nerve to the abductor digiti minimi muscle is not easily detectable on sonography, atrophy and fat replacement of the muscle from chronic denervation are readily recognized as a small hyperechoic muscle (Figure 13). Comparison with the adjacent muscles or the abductor digiti minimi muscle on the contralateral side may aid in determining atrophic changes. Routine scanning of this muscle is important during the sonographic evaluation of plantar fascioptthy. Nevertheless, evidence of chronic denervation of the abductor digiti minimi muscle has been reported to occur without symptoms; thus, it is important to interpret these findings in the clinical setting.[26]

Plantar Vein Thrombosis

Plantar vein thrombosis is an uncommon cause of plantar foot pain but should be in the differential diagnosis, particularly in the setting of sudden onset of plantar foot pain with associated soft tissue edema.[27,28] Characteristic findings include one or more enlarged veins that contain hypoechoic noncompressible material or a thrombus and absence of flow on color Doppler imaging (Figure 14).[27,29]

Anterior Tibialis Enthesopathy

Enthesopathy of the anterior tibialis tendon at its insertion onto the medial and plantar cortex of the medial cuneiform can produce pain in the medial plantar aspect of the foot. Sonography of insertional tendinopathy reveals a thickened hypoechoic tendon at its insertion with underlying cortical irregularity of the navicular and medial cuneiforms.[7] Tendinopathy mainly affects the plantar component of the tendon, while the dorsal component can appear normal (Figure 15).

Figure 12. Fusocellular sarcoma adjacent to the medial plantar nerve. **A** and **B**, Short-axis sonograms of the medial tarsal tunnel show the medial plantar nerve (black arrowheads) sandwiched between the sustentaculum tali (ST) and the well-demarcated hypoechoic mass (asterisk), indicating fusocellular sarcoma. The tumor is inferior to the posterior tibialis tendon (open arrow) and the flexor digitorum longus tendon (white arrow). Note the presence of color Doppler flow at the periphery of the tumor in **B** (white arrowhead). **C**, Coronal gadolinium-enhanced T1-weighted MR image from the same patient shows irregular enhancement of the tumor (asterisk). The open arrow indicates posterior tibialis tendon; and white arrow, flexor digitorum longus tendon.

A

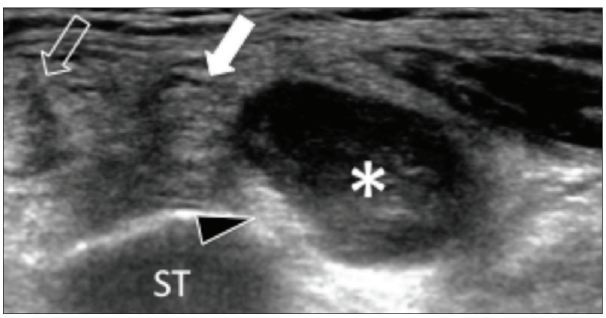

B

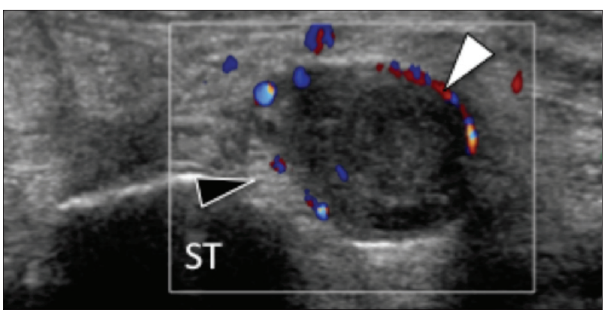

C

Rupture of the Flexor Hallucis Longus Tendon

The flexor hallucis longus tendon is the most posterior of the 3 tendons that traverse the medial tarsal tunnel. On sonography, it is easily identified during its course from the posterior talus to the insertion onto the distal phalanx of the great toe. Injury to this tendon at the distal tarsal tunnel or the plantar aspect of the foot is often experienced as plantar foot pain and should be a part of the routine sonographic evaluation of plantar foot pain (Figure 16). Dynamic examination during passive movements of the interphalangeal joint of the great toe allows differentiation from partial and complete tears.

Tears of the Distal Peroneus Longus Tendon

The peroneus longus tendon at the level of the cuboid tunnel frequently contains a small sesamoid bone, the os peroneum.[30] Tears of the peroneus longus tendon often result from a sudden contraction of the muscle from an inversion dorsiflexion injury. When the tear occurs at a plantar location, proximal displacement of the os peroneum results from contraction of the peroneus longus muscle. Although sonographic assessment of the peroneus longus tendon at the plantar aspect of the foot may be challenging, depiction of proximal migration of the os peroneum is not difficult and represents definitive evidence of a complete tear of the distal peroneus longus tendon (Figure 17).[31]

Foreign Bodies

Foreign bodies of the plantar aspect of the foot are not uncommon, and sonography can often identify a radiolucent foreign body such as wood, thorns, plastic, and small glass fragments with low lead content.[32] In addition, sonography is useful for assessing the size and position of a foreign body in relation to adjacent anatomic structures. Careful systematic scanning is necessary to identify small foreign bodies, and areas of edema and interruption of the architecture of the plantar fat pad may serve as clues to their location (Figure 18). Foreign bodies typically appear as linear hyperechoic structures often surrounded by a hypoechoic halo due to a granuloma or inflammatory reaction.[33] Surrounding hyperemia on color Doppler evaluation is also common. In general, wood, thorns, and plastic will usually show posterior acoustic shadowing, whereas metal and glass commonly show a reverberation artifact.[32]

Figure 13. Fat infiltration of the abductor digiti minimi muscle due to chronic compression of the first branch of the lateral plantar nerve. **A**, Coronal T1-weighted MR image shows fatty replacement of the abductor digiti minimi muscle (ADM) lateral to the normal-appearing flexor digitorum brevis muscle (FDB). Also shown are the quadratus plantae muscle (QP) and abductor hallucis muscle (AH). **B** and **C**, Short-axis sonogram of the affected foot (**B**) corresponding to **A** and the contralateral foot for comparison (**C**). In **B**, the sonogram shows a hyperechoic abductor digiti minimi muscle (black arrowheads), indicative of fatty replacement. In **C**, the contralateral side shows the normal echo texture of the abductor digiti minimi muscle (white arrowheads).

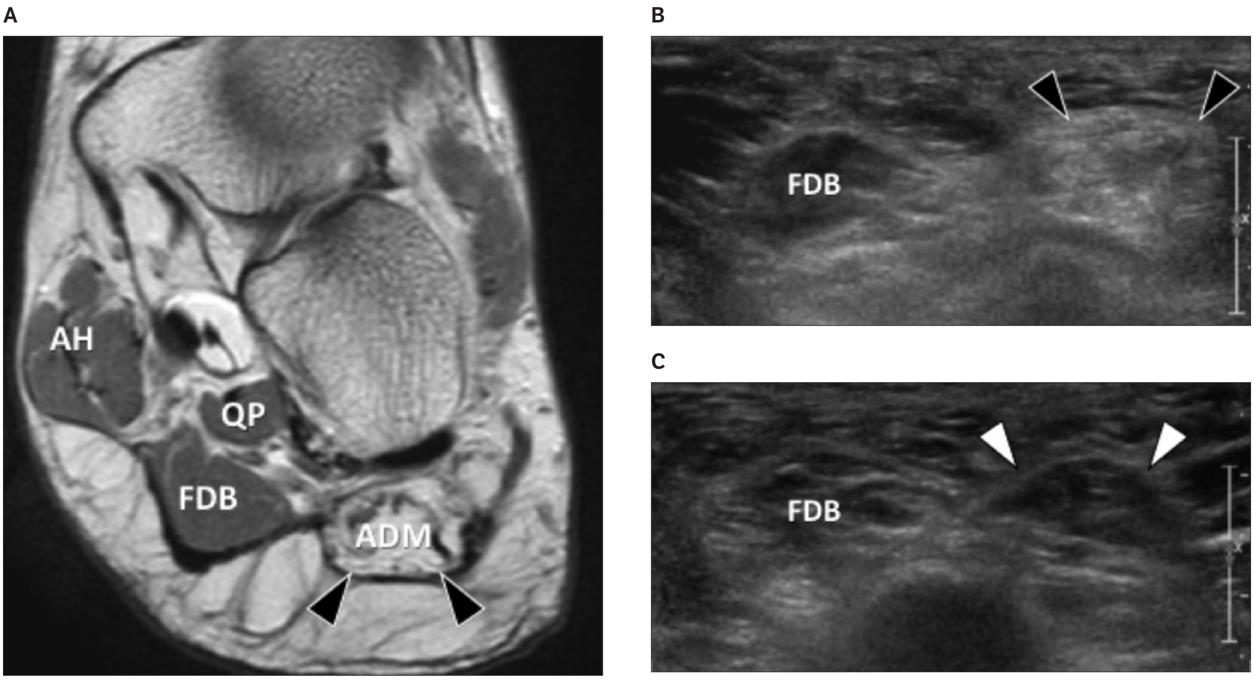

Figure 14. Plantar vein thrombosis. **A** and **C**, Short-axis sonograms of the plantar foot without (**A**) and with (**C**) compression. In **A**, the sonogram shows the patent medial plantar veins (white arrowheads), the enlarged lateral plantar vein containing a hypoechoic thrombus (black arrowhead), and the normal medial plantar artery (curved white arrow). In **C**, the lateral thrombosed plantar vein is noncompressible (black arrowhead). **B**, Long-axis sonogram of the lateral plantar vein (corresponding to the black arrowhead in **C**) shows an enlarged vein filled with a hypoechoic clot (black arrowheads). **D**, Short-axis color Doppler sonogram of the lateral plantar vein (corresponding to the black arrowheads in **B**) shows no flow signal inside the vein (white arrowhead) with flow inside the adjacent lateral plantar artery.

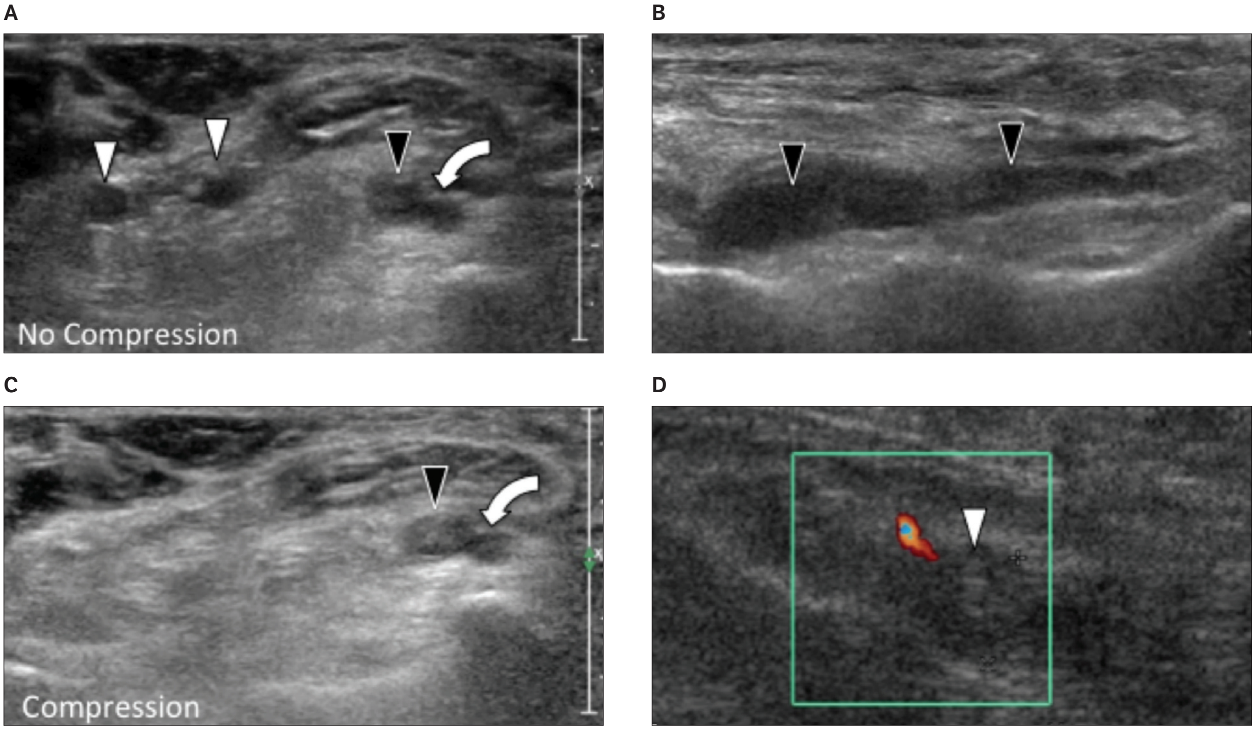

Figure 15. Enthesopathy of the tibialis anterior tendon. **A**, Short-axis sonogram of the distal portion of the anterior tibialis tendon shows a normal dorsal component (white arrowhead) and a swollen hypoechoic irregular plantar component (black arrowhead). **B** and **C**, Long-axis sonograms of the plantar (**B**) and dorsal (**C**) components show an enlarged tendon with loss of the normal fibrillar echo texture (black arrowheads) in **B** and the normal tendon echo texture (white arrowheads) in **C**.

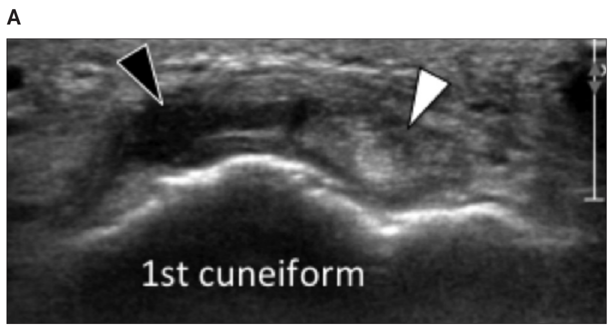

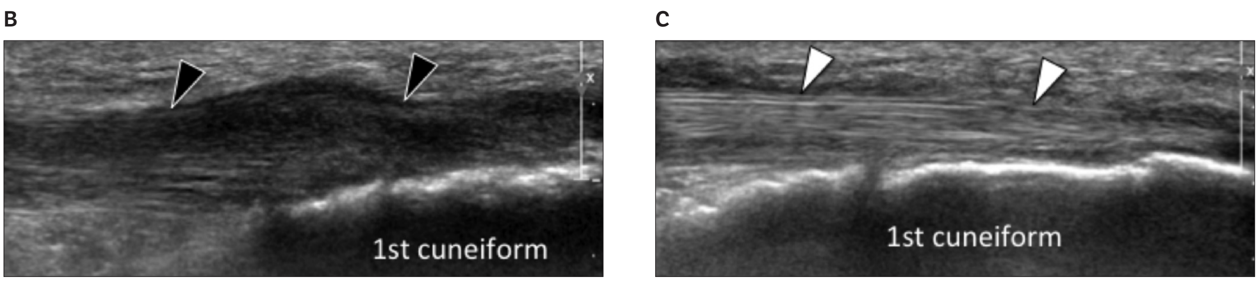

A

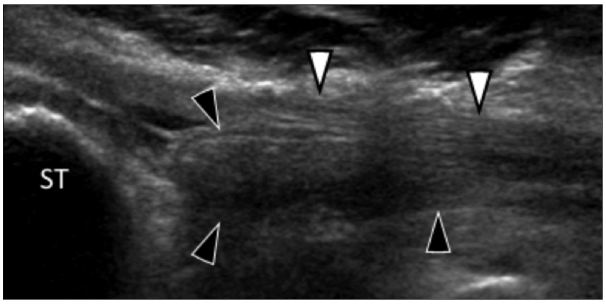

Figure 16.Rupture of the flexor hallucis longus tendon. **A**, Long-axis sonogram of the medial ankle shows the distal stump of the torn flexor hallucis longus tendon (black arrowheads), which lies distal to the sustentaculum tali (ST) and adjacent to the normal flexor digitorum longus tendon (white arrowheads). **B**, Corresponding sagittal T2-weighted MR image shows the torn flexor hallucis longus tendon (black arrowheads) just distal to the sustentaculum tali. **C**, More medial MR image shows the normal flexor digitorum longus tendon (white arrowhead).

B C

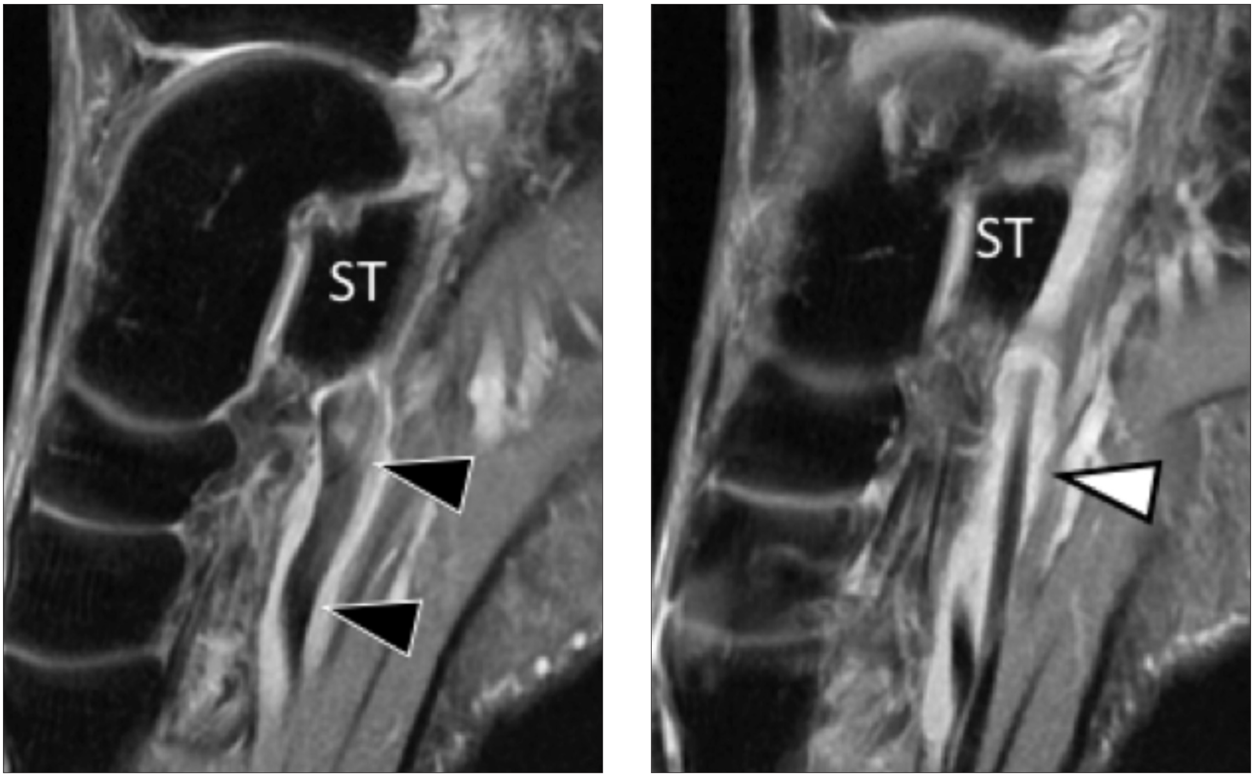

Figure 17. Complete tear of the peroneal longus tendon with proximal dislocation of the os peroneum. **A**, Long-axis sonogram obtained at the lateral aspect of the calcaneum shows the proximally dislocated sesamoid bone (black arrows). Note the distal tendon stump (black arrowheads). **B**, External oblique radiograph confirms the proximal dislocation of the os peroneum (black arrow). Dashed arrows indicate the direction of the dislocation.

A B

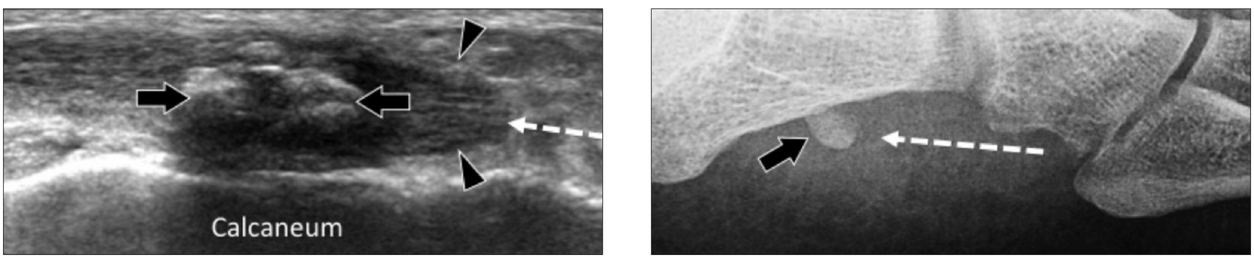

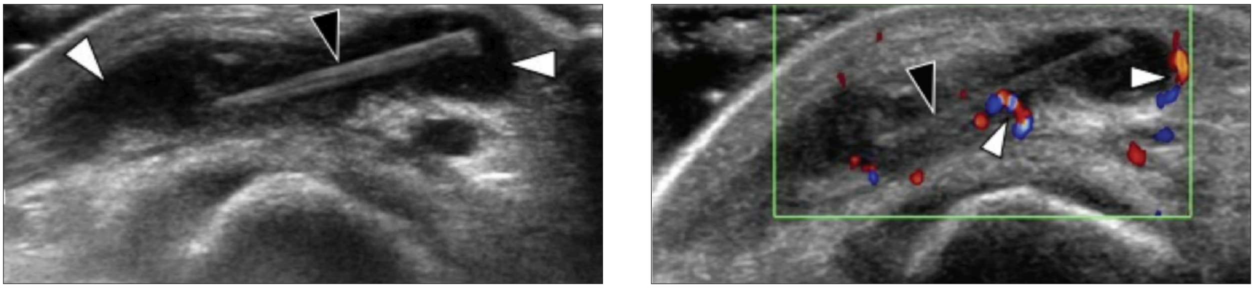

Figure 18. Foreign body embedded in the calcaneal fat pad. **A** and **B**, Coronal grayscale (**A**) and color Doppler (**B**) sonograms of the plantar fat pad show a hyperechoic wood splinter (black arrowheads) with surrounding edema (white arrowheads). Note the presence of hypervascular changes in **B** (white arrowheads), suggestive of a reactive inflammatory response.

Sonography is invaluable for guiding removal of the foreign body or preoperative planning by marking the skin, assessing the depth of the fragment, and identifying adjacent neurovascular structures.

Conclusions

Plantar foot pain is a common musculoskeletal condition. High-resolution sonography is an excellent imaging modality for visualizing the abnormalities characteristic of plantar fasciopathy, the most common cause of plantar foot pain, as well as assessing other structures in the differential diagnosis. Sonography is a readily available, economical, and dynamic tool that, together with conventional radiography, allows for an excellent assessment of the different disorders that cause plantar foot pain.

References

1. Hill CL, Gill TK, Menz HB, Taylor AW. Prevalence and correlates of foot pain in a population-based study: the North West Adelaide health study. *J Foot Ankle Res* 2008; 1:1–7.
2. Thomas MJ, Roddy E, Zhang W, Menz HB, Hannan MT, Peat GM. The population prevalence of foot and ankle pain in middle and old age: a systematic review. *Pain* 2011; 152:2870–2880.
3. Hannan MT, McLennan CE, Rivinus MC, et al. Population-based study of foot disorders in men and women from the Framingham Study [abstract]. *Arthritis Rheum* 2006; 54(suppl):S497.
4. Riddle DL, Schappert SM. Volume of ambulatory care visits and patterns of care for patients diagnosed with plantar fasciitis: a national study of medical doctors. *Foot Ankle Int* 2004; 25:303–310.
5. Sabir N, Demirlenk S, Yagci B, Karabulut N, Cubukcu S. Clinical utility of sonography in diagnosing plantar fasciitis. *J Ultrasound Med* 2005; 24:1041–1048.
6. McNally EG, Shetty S. Plantar fascia: imaging diagnosis and guided treatment. *Semin Musculoskelet Radiol* 2010; 14:334–343.
7. Bianchi S, Martinoli C. Foot. In: Bianchi S, Martinoli C (eds). *Ultrasound of the Musculoskeletal System*. Berlin, Germany: Springer-Verlag; 2007:835–888.
8. Karabay N, Toros T, Hurel C. Ultrasonographic evaluation in plantar fasciitis. *J Foot Ankle Surg* 2007; 14:442–446.
9. Ieong E, Afolayan J, Carne A, Solan M. Ultrasound scanning for recalcitrant plantar fasciopathy. Basis of a new classification. *Skeletal Radiol* 2013; 42:393–398.
10. Lemont H, Ammirati KM, Usen N. Plantar fasciitis: a degenerative process (fasciosis) without inflammation. *J Am Podiatr Med Assoc* 2003; 93:234–237.
11. Walther M, Radke S, Kirschner S, Ettl V, Gohlke F. Power Doppler findings in plantar fasciitis. *Ultrasound Med Biol* 2004; 30:435–440.
12. Louwers MJ, Sabb B, Pangilinan PH. Ultrasound evaluation of a spontaneous plantar fascia rupture. *Am J Phys Med Rehabil* 2010; 89:941–944.
13. Griffith JF, Wong TY, Wong SM, Wong MW, Metreweli C. Sonography of plantar fibromatosis. *AJR Am J Roentgenol* 2002; 179:1167–1172.
14. Widmann G, Riedl A, Schoepf D, Glodny B, Peer S, Gruber H. State-of-the-art HR-US imaging findings of the most frequent musculoskeletal soft-tissue tumors. *Skeletal Radiol* 2009; 38:637–649.
15. Arni D, Lambert V, Delmi M, Bianchi S. Insufficiency fracture of the calcaneum: sonographic findings. *J Clin Ultrasound* 2009; 37:424–427.
16. Bodner G, Stöckl B, Fierlinger A, Schocke M, Bernathova M. Sonographic findings in stress fractures of the lower limb: preliminary findings. *Eur Radiol* 2005; 15:356–359.
17. Hendrix CL, Jolly GP, Garbalosa JC, Blume P, DosRemedios E. Entrapment neuropathy: the etiology of intractable chronic heel pain syndrome. *J Foot Ankle Surg* 1998; 37:273–279.
18. Lau JT, Daniels TR. Tarsal tunnel syndrome: a review of the literature. *Foot Ankle Int* 1999; 20:201–209.
19. Nagaoka M, Matsuzaki H. Ultrasonography in tarsal tunnel syndrome. *J Ultrasound Med* 2005; 24:1035–1040.

20. Stormont DM, Perterson HA. The relative incidence of tarsal coalition. *Clin Orthop Relat Res* 1983; 181:28–36.
21. Newman JS, Newberg AH. Congenital tarsal coalition: multimodality evaluation with emphasis on CT and MR imaging. *Radiographics* 2000; 20:321–332.
22. Nagaoka M, Satou K. Tarsal tunnel syndrome caused by ganglia. *J Bone Joint Surg Br* 1999; 81:607–610.
23. Pham H, Fessell DP, Femino JE, Sharp S, Jacobson JA, Hayes CW. Sonography and MR imaging of selected benign masses in the ankle and foot. *AJR Am J Roentgenol* 2003; 180:99–107.
24. Yamamoto T, Mizuno K. Tarsal tunnel syndrome caused by synovial sarcoma. *J Neurol* 2001; 248:433–434.
25. Chundru U, Liebeskind A, Seidelmann F, Fogel J, Franklin P, Beltran J. Plantar fasciitis and calcaneal spur formation are associated with abductor digiti minimi atrophy on MRI of the foot. *Skeletal Radiol* 2008; 37:505–510.
26. Oztuna V, Ozge A, Eskandari MM, Colak M, Gölpinar A, Kuyurtar F. Nerve entrapment in painful heel syndrome. *Foot Ankle Int* 2002; 23:208–211.
27. Siegal DS, Wu JS, Brennan DD, Challies T, Hochman MG. Plantar vein thrombosis: a rare cause of plantar foot pain. *Skeletal Radiol* 2008; 37:267–269.
28. Bernathova M, Bein E, Bendix N, Bodner G. Sonographic diagnosis of plantar vein thrombosis: report of 3 cases. *J Ultrasound Med* 2005; 24:101–103.
29. Barros MV, Labropoulos N, Plantar vein thrombosis: evaluation by ultrasound and clinical outcome. *Angiology* 2010; 61:82–85.
30. Peacock KC, Resnick EJ, Thoder JJ. Fracture of the os peroneum with rupture of the peroneus longus tendon: a case report and review of the literature. *Clin Orthop Relat Res* 1986; 202:223–226.
31. Brigido MK, Fessell DP, Jacobson JA, et al. Radiography and US of os peroneum fractures and associated peroneal tendon injuries: initial experience. *Radiology* 2005; 237:235–241.
32. Valle M, Zamorani MP. Skin and subcutaneous tissue. In: Bianchi S, Martinoli C (eds). *Ultrasound of the Musculoskeletal System.* Berlin, Germany: Springer-Verlag; 2007:27–31.
33. Wortsman X. Common applications of dermatologic sonography. *J Ultrasound Med* 2012; 31:97–111.